

TeV J2032+4130: a not-so-dark Accelerator?

Y. M. Butt¹, J. A. Combi², J. Drake¹, J. P. Finley³, A. Konopelko³, M. Lister³, J. Rodriguez⁴

¹ *Harvard-Smithsonian Center for Astrophysics, 60 Garden St., Cambridge, MA 02138, USA*

² *Departamento de Física (EPS), Universidad de Jaén, Campus Las Lagunillas s/n, 23071 Jaén, SPAIN*

³ *Department of Physics, Purdue University, West Lafayette, IN 47907, USA*

⁴ *CEA Saclay, DSM/DAPNIA/SaP, F-91191 Gif sur Yvette, FRANCE*

Abstract

The HEGRA gamma-ray source TeV J2032+4130 is considered the prototypical “dark accelerator”, since it was the first TeV source detected with no firm counterparts at lower frequencies. The Whipple collaboration has observed this source in 2003-5 and those data indicate that the Whipple TeV emission hotspot is displaced about 9 arcminutes to the northeast of the HEGRA position. Here we report on a dual-lobed non-thermal radio source that appears in the Westerbork Synthesis Radio Telescope (WSRT) dataset consistent with the locations of the Whipple and, to a lesser extent, also the HEGRA hotspot. A weak diffuse non-thermal radio condensation exists ~5 arcmin to the SW of this source, along the axis of the lobes and thus may be related. We also find a weak non-thermal shell-like SNR-type object, with a location and morphology very similar to the HEGRA source, in archival VLA data at 4.8 GHz. Thus, either of these objects – or perhaps even both – may be viable counterparts of the reported very high energy (VHE) gamma-ray emissions in this region. If so, TeV J2032+4130 may not be a “dark accelerator” after all. Further observations with the new generation of imaging Cherenkov telescopes are needed to pin down the location and morphology of the TeV emission region and thus clear up the confusion over its possible lower frequency counterparts.

Introduction

In 2002 the HEGRA collaboration reported on a steady and extended (~ 6.2 arcmin radius) TeV gamma-ray emitting region, TeV J2032+4130, near the massive stellar association Cygnus OB2 (Aharonian et al., 2002, 2005). We followed-up this source using the VLA and CHANDRA, but found no obvious counterparts at the lower frequencies (Butt et al., 2003, 2006; Mukherjee et al., 2003, 2006). Paredes et al. (2006) have very recently reported on some deeper radio observations which do show a handful of very interesting potential counterparts. Several possible origins of the gamma-ray emission have been suggested in the literature having to do, variously, with the termination lobes of Cyg X-3 (Aharonian et al., 2002; see also, Marti, Paredes & Peracaula 2000); the stellar winds in Cyg OB2 (Aharonian et al., 2002; Butt et al., 2003; 2006; Domingo-Santamaria & Torres, 2006); a possible proton-blazar (Mukherjee et al., 2003); a pulsar wind nebula (Bednarek 2003; 2006); or possible microquasars (Paredes et al., 2006). However, since none of these possible scenarios has yet been conclusively verified, this, and other similar TeV sources without firm counterparts, have been dubbed “dark accelerators” by some authors. It is commonly believed that they are most likely of hadronic origin. TeV J2032+4130, being the first discovered is, in fact, the prototype of this informal class of sources.

Using archival 10m data from 1989-90, the Whipple collaboration confirmed the existence of TeV J2032+4130 (Lang et al., 2004), and more recently a total of 65.5 hr of Whipple data taken during 2003-2005 towards this source has been reported (Konopelko et al. 2006). The analysis of the latest dataset reveals a distinct excess in the field of view at a significance of 6σ . The centroid position of this γ -ray source is $\alpha=20^{\text{h}}32^{\text{m}}27^{\text{s}}$, $\delta=41^{\circ}39'17''$ and the estimated integral flux is about 8% of the Crab-Nebula flux. The data are consistent with a point-like source, even though an extended source with an effective radius less than $7'$ cannot be ruled out. The center of gravity of the γ -ray emission as seen in the Whipple data is about 9 arcmin northeast of that reported by HEGRA. However, given the statistical and systematic uncertainties in the source localization, which are $\sim 4'$ and $6'$, respectively, the Whipple hotspot location can be considered consistent with the HEGRA γ -ray source position [Fig. 1a].

Though no obvious point-like or extended radio counterparts were found at the location of the extended HEGRA source in VLA data (Butt et al., 2003), we noted two non-thermal radio sources with a jet-like structure marginally coincident with the HEGRA position in the

Westerbrok Synthesis Radio Telescope (WSRT) data reported by Setia-Guawan et al. (2003) [hereafter SG2003] at 350 MHz and 1.4 GHz (see Table 3 in Butt et al., 2006; hereafter B2006).

Though we pointed out these non-thermal radio sources in B2006 we did not then consider them strong candidate counterparts of TeV J2032+4130 due to their marginal positional coincidence with the HEGRA hotspot. However, since the new Whipple data indicate that the TeV emission centroid position may be displaced significantly north relative to the HEGRA position, these two radio sources now appear to be much more promising counterparts of the TeV source. We emphasize that both the HEGRA and the Whipple TeV emission regions agree with the location of these radio sources, within the respective errors quoted (Aharonian et al., 2005; Konopelko et al. 2006).

Radio Analysis

We reanalyzed the WSRT data of SG2003 using standard procedures with the AIPS package of the National Radio Astronomy Observatory (NRAO). For these observations the WSRT beam size at 1.4GHz and 350 MHz was 13'' \times 19'' and 48'' \times 75'' respectively. The limiting flux-densities were \sim 2mJy at 1.4GHz and \sim 7mJy at 350MHz. We convolved the radio map at 1420 MHz with a similar synthesized beam as the 350 MHz observations in order to perform the spectral index measurements.

We independently recalculated the intensities and spectral indices of the dual-lobed radio structure and found that they agree with the values stated by SG2003 (Table 1).

# (SG2003)	Position (J2000)	1.4GHz Flux Density	350MHz Flux Density	Sp. Index
217	20 32 1.22, +41 37 13.64	36 \pm 5 mJy	87 \pm 5 mJy	-0.65
218	20 32 2.16, +41 37 59.24	39 \pm 5 mJy	122 \pm 3 mJy	-0.84

Table 1: Characteristics of the non-thermal dual-lobe radio object found in WSRT data.

Furthermore, we confirmed the existence of this non-thermal radio source in archival VLA¹ (NVSS) and in Canadian Galactic Plane Survey² (CGPS) data at 1.4GHz and 408 MHz. (In fact, this source has been cataloged as a single object, NVSS J203201+413722 in the NVSS catalog.)

¹ The archives can be accessed via: www.nrao.edu

² The CGPS data can be accessed via: www1.cadc-ccda.hia-ihp.nrc-cnrc.gc.ca/cgps/query.html

There is also a weak diffuse non-thermal radio condensation roughly aligned with the axis of the lobes located ~ 5 arcmin further SW of the dual-lobed jet-like source, but it is unknown whether the structures are related (Fig. 2). This radio source is located at $\alpha_{2000}, \delta_{2000} \sim (20\ 31\ 53, +41\ 32\ 35)$ and has a 365MHz flux of ~ 11.6 mJy. At 1400MHz, the source is so weak that it is only marginally above the noise level of ~ 2 mJy. The spectral index of this radio emission is -1.3 ± 0.5 .

We also found two other non-thermal radio sources in the extended radio field, one of which is also dual-lobed. However, the locations of these sources are inconsistent with the position of either one or both TeV gamma-ray hotspots, and therefore we do not consider them likely counterparts of the TeV emission (Fig. 1a). The Eastern radio source has two lobes, with Lobe 1 located at $\alpha_{2000}, \delta_{2000} = (20\ 33\ 22.496 \pm 0.011, +41\ 27\ 26.04 \pm 0.18)$ with 1400 MHz flux density $F(1400) \sim 29.1$ mJy, and Lobe 2 located at $\alpha_{2000}, \delta_{2000} = (20\ 33\ 24.57 \pm 0.012, +41\ 27\ 17.55 \pm 0.28)$ with $F(1400) \sim 19.2$ mJy. At 350MHz the two sources blend into one due to the poorer resolution with a total 350 MHz flux density of, $F(350) \sim 105.7$ mJy. This extended source was also noted by Wendker, Higgs and Landecker (1991) as “19P26” and by Taylor et al. (1996) as WSRTGP 2031+4116. The other, more northern, non-thermal radio source is located at $\alpha_{2000}, \delta_{2000} = (20\ 33\ 10.975 \pm 0.011, +41\ 42\ 13.2 \pm 0.178)$ with flux densities, $F(1400) \sim 23.4$ mJy and $F(350) \sim 86.1$ mJy. This source was cataloged by Taylor et al. (1996) as WSRTGP 2031+4131 and is about 5 arcsec from star #419 in the compilation of Massey & Thompson (1991).

For completeness, we also estimated the total diffuse radio flux in the extended radio emission region coincident with the Whipple hotspot. We considered all the radio flux with the elliptical region shown in Fig. 1, except for that due to the dual-lobed radio source. We found the following flux densities at the two frequencies for the diffuse radio emission in this region: $F(350\text{ MHz}) = 2.1 \pm 0.3$ Jy and $F(1420\text{ MHz}) = 2.8 \pm 0.4$ Jy.

Lastly, we also reanalyzed the same archival VLA data presented by Paredes et al. (2006) at 1.4 and 4.8GHz. In addition to confirming the half-arc structure they report at 1.4GHz, we find a weak, although fairly well-formed, shell-like structure reminiscent of a supernova remnant at 4.8GHz in the region of the HEGRA source. This structure has an approximate radius of 5 arcmin, which is consistent with the reported extension of the HEGRA source (Fig 3). The

emission is weak, with a total 4.8GHz flux of just ~ 15 mJy, and at 1.4GHz only the western part of the full ring-like structure is evident. The radio spectral index is variable across the structure and ranges from $\alpha \sim -1.8 \pm 0.2$ in the south, to $\sim -1 \pm 0.2$ in the west, to $\sim +0.8$ or larger in the east, as shown in Fig 3. We can thus tentatively say that the western and southern regions of this object are more non-thermal than the rest of the structure. This radio ring is not evident in the 365 MHz WSRT data but this may be due to that interferometer being optimized for higher-resolution at the expense of diffuse sensitivity. Deeper, more sensitive observations of this region at a handful of radio frequencies would be very useful to extract higher-fidelity data on this interesting structure.

Chandra

A Chandra X-ray Observatory ACIS-I observation of the region in the vicinity of TeV J2032+4131 was described by B2006. Here, we reanalyzed the same 48728s exposure. Analysis was performed using the Chandra Interactive Analysis of Observations (CIAO) software Version 3.3.0.1. B2006 listed sources found by an automated wavelet-base source detection algorithm (implemented in CIAO as the utility *wavedetect*), and three sources from that list that fall close to the radio source: 36, 153 and 227 (Src#227 is the same as Source 1 of Mukherjee et al., 2003). Of these, 36 and 153 are faint while 227 is a bright source with a count rate of about 0.015 count/s. Their positions are as follows:

B2006 Src #36 (E in Fig. 1)	$\alpha_{2000}, \delta_{2000} = (20\ 32\ 03.12, +41\ 38\ 23.64)$
B2006 Src #153 (F in Fig. 1)	$\alpha_{2000}, \delta_{2000} = (20\ 31\ 58.32, +41\ 36\ 48.60)$
B2006 Src #227 (G in Fig. 1)	$\alpha_{2000}, \delta_{2000} = (20\ 31\ 56.39, +41\ 37\ 22.43)$

In addition to these sources, we also located by eye two additional regions of enhanced X-ray brightness that appear to be slightly more extended than a point source due to the effects of point spread function (psf)-distortion this far off-axis. One of these falls between the two radio lobes but is off-set slightly east of their centre; the other is coincident with the southern radio lobe. These two regions of enhanced X-ray brightness can each be described by two positions derived from a $8 \times$ binned image of the field:

Central: (A in Fig. 1)	$\alpha_{2000}, \delta_{2000} = (20\ 32\ 02.4, +41\ 37\ 37)$
(B in Fig. 1)	$\alpha_{2000}, \delta_{2000} = (20\ 32\ 02.1, +41\ 37\ 34)$

Southern-lobe: (**C** in Fig. 1) $\alpha_{2000}, \delta_{2000} = (20\ 32\ 01, +41\ 37\ 10.6)$
(**D** in Fig. 1) $\alpha_{2000}, \delta_{2000} = (20\ 32\ 00.6, +41\ 37\ 06.7)$

We find that these 2 regions are both rather hard, containing more counts in the 2-10keV band than in the 0.5-2keV one.

The diffuse non-thermal radio condensation located ~ 5 arcmin SW of the dual-lobed source also has two X-ray sources coincident with its location: SW Condensation X1: $\alpha_{2000}, \delta_{2000} = (20\ 31\ 52.71, +41\ 32\ 40.20)$ and SW Condensation X2: $\alpha_{2000}, \delta_{2000} = (20\ 31\ 52.49, +41\ 32\ 09.43)$. The first is likely the X-ray counterpart of star #157 of Massey & Thompson (1991) at $\alpha_{2000}, \delta_{2000} = (20\ 31\ 52.63, +41\ 32\ 40.7)$, whereas the second could truly be a X-ray counterpart of the radio condensation. The X-ray event characteristics of all these sources nearby or coincident with the relevant radio structures are listed in Table 2 including the total counts within the source region, the source signal-to-noise ratio, and the relative fractions of observed counts that fell into the energy ranges 0.5-2.5 keV and 2.5-10 keV.

In the case of the bright source 227 (**G** in Fig 1b), we also performed spectral fitting using the CIAO *Sherpa* fitting engine. The data are well-represented (reduced $\chi^2=0.33$ for 133 degrees of freedom) by a power law with photon index $\alpha=1.4\pm0.3$ absorbed by a medium described by a hydrogen column density of $2.0\pm0.4\times10^{22}\text{ cm}^{-2}$. The flux for this source is $\sim 4\times10^{-13}\text{ ergs cm}^{-2}\text{ s}^{-1}$.

<i>X-ray Source</i>	Cts*	S/N	Frac. 0.5-2.5 keV	Frac. 2.5-10 keV	X-ray Flux ($\text{erg cm}^2\text{ s}^{-1}$)
Central: A&B	32	2.8	0.28	0.72	$\sim 1.8\times 10^{-14}$
South-lobe: C&D	47	2.6	0.38	0.62	$\sim 2.6\times 10^{-14}$
SW condensation X1	9	2.9	0.89	0.11	$\sim 5\times 10^{-15}$
SW condensation X2	9	2.8	0.56	0.44	$\sim 5\times 10^{-15}$
B2006:36 E	24	2.3	0.38	0.62	$\sim 1.3\times 10^{-14}$
B2006:153 F	29	2.5	0.48	0.52	$\sim 1.6\times 10^{-14}$
B2006:227 G	718	26.0	0.31	0.69	$\sim 4\times 10^{-13}$
Background	-	-	0.29	0.71	-

Table 2: Characteristics of Chandra sources detected nearby or coincident with the non-thermal dual-lobe radio object. Note that the lobe sources are both rather hard in X-rays.

* *total counts in source region (ie source + background)*

Infrared and Optical

At the very center of the radio structure, coincident with the X-ray emission of sources **A** & **B**, lies a 2MASS infrared source, 2MASS 20320186+4137377, with standard magnitudes $J=16.401\pm0.107$, $H=15.325\pm0.096$ and $K=14.879$. With the present available information, however, it is impossible to tell if this object is stellar or not, since a spectrum is not available. There are also several other 2MASS sources nearby or coincident with the radio lobes, as shown in Fig 1b, but it is unclear if these are related to this source.

We inspected the USNO-B1.0 catalog (Monet et al., 2003), but found no objects coincident with the central 2MASS source at optical wavelengths. However there is a star at: $\alpha_{2000}, \delta_{2000} = (20\ 32\ 00.1, +41\ 37\ 14)$ with $B_{\text{mag}}=15.46$, $V_{\text{mag}}=14.00$ (Star #179 in Massey & Thompson 1991), marginally coincident with the southern lobe of the radio structure. This star is also designated GSC 03161-00887.

Hard X-ray

We have examined 625ksec co-summed data of the IBIS detector aboard the INTEGRAL satellite towards Cygnus, and find no positive detection of TeV J2032+4130 in the 20-300keV band. We derive the following 3σ upper limits: 20-40 keV : 0.85 mCrab; 40-80 keV : 1.8 mCrab; 80-150 keV: 4.8 mCrab; 150-300 keV: 110 mCrab

Discussion & Conclusions

Motivated by the more northerly location of the center-of-gravity of Whipple hotspots (Lang et al. 2004; Konopelko et al., 2006) for the source TeV J2032+4130, as compared with the HEGRA one (Aharonian et al., 2002; 2005) we undertook a multiwavelength study of that region in pursuit of possible lower frequency counterparts of the high-energy emission observed.

We find a dual-lobed non-thermal radio object consistent with the position of the Whipple hotspot, and to a lesser extent, also the HEGRA TeV emission region³. There is a 2MASS

³ The HEGRA source is described as having COG $\alpha_{2000} = 20\text{hr } 31\text{m } 57.0\text{s} \pm 6.2\text{s stat} \pm 13.7\text{s sys}$; $\delta_{2000} = 41^\circ 29' 56.8'' \pm 1.1' \text{stat} \pm 1.0' \text{sys}$ and extension (standard deviation of the 2DGaussian fit) as

infrared source (2MASS 20320186+4137377) and coincident X-ray emission (sources **A** & **B**) at the center of this radio structure. The latter could be a signature of X-ray emission from nearby the putative compact object or disk emission. At least the southern radio lobe also appears to emit in X-rays, and quite possibly the northern one also. Both the central and southern lobe X-ray sources appear to have a hard spectrum, such as may be expected from an absorbed source, but the statistics are poor (Table 2). The X-ray emission from the lobe(s) might be the result of fast shocks that travel along the radio jet, heating the gas up to very high temperatures. There is also a weak diffuse non-thermal radio source roughly aligned with the axis of the lobes and located about 5 arcmin SW [$\alpha_{2000}, \delta_{2000} = (20\ 31\ 53, +41\ 32\ 35)$ with a 365MHz flux of ~ 11.6 mJy, see Fig. 2], but it is unknown whether the structures are related. This source is notable since it is located within the HEGRA emission region, and is also diffuse. If this source is a TeV emitter, in addition to the suggested dual-lobed jet-like object, then it is possible that the extension reported by HEGRA (and not ruled out by Whipple) arises from the composite nature of these two emission regions.

With the information available we cannot yet make a definitive statement on the nature of the dual-lobed jet-like non-thermal radio source. If Galactic, it could well be a microquasar (eg. Bosch-Ramon, Aharonian and Paredes, 2005; Paredes 2006) or, less likely, pulsar-related (eg. Bednarek, 2006); if extragalactic, it is most likely a so-called “double-double” radiogalaxy with powerful dual radio cocoons (eg. Schoenmakers 2001). M87 and Centaurus A are examples of TeV- and GeV-emitting non-blazar radiogalaxies, respectively (eg. Grindlay et al., 1975; Sreekumar et al., 1999; Beilicke et al, 2005; Combi et al., 2003); however, at least in the case of M87, the VHE emission appears to be point-like (Aharonian et al., 2006).

To better discriminate between the Galactic vs. extragalactic alternative one would need to detect the central object at optical and/or IR frequencies and obtain a spectrum to be able to test for the possible redshift of the H-alpha or other emission lines. If no redshift is found it would of course imply that this source is Galactic, possibly similar to a number of highly-absorbed INTEGRAL sources recently discovered (eg. Filliatre & Chaty, 2004; Chaty & Rahoui, 2006). Further TeV observations and multiwavelength monitoring of this radio structure is clearly warranted and could be very useful in determining its true nature.

$\sigma_{src} = 6.2' \pm 1.2'_{stat} \pm 0.9'_{sys}$ (Aharonian et al. 2005). Thus the radio source whose center is roughly at $(\alpha_{2000}, \delta_{2000}) \sim (20\ 32\ 02, +41\ 37\ 34)$ is consistent with the HEGRA position.

Besides the dual-lobed source, relatively strong extended radio emission is also present within the area of the Whipple hotspot, $F(350 \text{ MHz}) = 2.1 \pm 0.3 \text{ Jy}$ and $F(1420 \text{ MHz}) = 2.8 \pm 0.4 \text{ Jy}$. Though this could also conceivably be a radio counterpart of the TeV emission, this extended radio emission is thermal in nature, with a mean index of 0.12 ± 0.1 . Furthermore, the extended thermal radio region lies well outside the HEGRA TeV J2032+4130 location. For these two reasons we disfavor its direct association with TeV J2032+4130.

We have discussed above the possible association of the dual-lobed radio structure, together with its plausibly related radio condensation 5 arcmin to the SW, with TeV J2032+4130. However, we emphasize that the case is far from closed. The alternate associations of this VHE source with possible microquasars (Paredes et al., 2006) or with an outlying sub-group of very massive and powerful stars in Cyg OB2 are also somewhat persuasive (see, eg., Fig 1 in Butt et al., 2003 and Fig. 3 in B2006). In fact, Anchordoqui et al. (2006a, 2006b) have recently proposed an interesting new hypothesis for the origin of the high energy flux in the latter scenario: they suggest that the TeV gamma-rays could result from the photo-deexcitation of PeV energy nuclei that are themselves the photo-disintegration products of heavier nuclei broken-up in a bath of intense ultraviolet photons, such as would be present in Cyg OB2. Other interesting phenomena, such as possible time-correlated supernovae of a previous generation of stars in the Cyg OB2 region – which may have led to the ejection of sets of binary pulsars (Vlemmings, Cordes and Chatterjee 2004) – may also be involved in untangling the true scenario of the origin of the TeV flux seen here.

VLA data at 4.8 GHz also hints at the presence of a weak ($\sim 15 \text{ mJy}$ at 4.8GHz) SNR-like object with a radius of about 5 arcmin which is consistent with the $\sim 6.2 \text{ arcmin } 1\sigma$ extension reported by HEGRA for TeV J2032+4130 (Fig. 3). The center of this ring-like structure is approximately $\alpha_{2000}, \delta_{2000} = (20 \text{ } 32 \text{ } 00, +41 \text{ } 29 \text{ } 30)$, also consistent with the HEGRA report and at least its western and southern parts are non-thermal. Assuming this object is co-located with Cyg OB2 at a distance of 1.7 kpc, its radius would be only $\sim 3 \text{ pc}$ and its age as low as ~ 500 years. Deeper radio observations at several frequencies are needed to pin down the nature of this very interesting source, especially to see whether or not it really is an SNR. This radio ring may also be due to multiple large-scale shocks created by several of the very powerful stars in Cyg OB2 (eg., Cesarsky & Montmerle, 1983). It remains to be seen whether this intriguing, dominantly non-thermal radio object may be related to the VHE gamma-ray emission.

A proper understanding of TeV J2032+4130 may also need to take into account the recent results from the air-shower arrays MILAGRO and TIBET, which have shown the entire Cygnus region to be a bright source of TeV gamma-rays (Atkins et al., 2005) and possibly also cosmic rays (Amenomori et al., 2006; Abdo et al., 2006).

Clearly it would be very helpful to better determine the true location and morphology of the TeV gamma-ray emission region (TeV J2032+4130) with higher precision. This is something the new generation of Imaging Cherenkov telescopes is ideally suited for doing. We estimate, for instance, that just 20hrs of VERITAS time could yield a 6 sigma detection with better systematics and allow one to localize this source, and, simultaneously, give better morphological information possibly confirming or denying its association with the various possible lower frequency counterparts in the region.

References

- Abdo, A., et al., 2006, ApJ Lett. submitted, astro-ph/0611691
- Aharonian, F., et al. 2002, A&A, 393, L37
- Aharonian, F. et al., 2005, A&A, 431, 197
- Aharonian, F., et al., Science Express, Oct 26, 2006:
<http://www.sciencemag.org/cgi/content/abstract/1134408v1>
- Anchordoqui, L. et al., 2006a, astro-ph/0611580
- Anchordoqui, L. et al., 2006b, astro-ph/0611581
- Amenomori, M., et al., 2006, Science, 314, 439 astro-ph/0610671
- Atkins, R., et al., 2005, Phys Rev Lett. 95, 1103
- Bednarek, W., 2003, MNRAS, 345, 847
- Bednarek, W., 2006, astro-ph/0610307, Proc. Multimessenger approach to high energy gamma-ray sources, 2006.
- Beilicke, M, et al., in Proceedings of the 29th ICRC. August 3-10, 2005, Pune, India. Volume 4, p.299. Available on-line: <http://icrc2005.tifr.res.in/htm/Vol-Web/Vol-14/14299-ger-beilicke-M-abs1-og23-oral.pdf>
- Bosch-Ramon, V., Aharonian, F., and Paredes, J. M., 2005, Contributed talk presented at the "Astrophysical Sources Of High Energy Particles and Radiation" conference, held in Torun, June 2005, AIP Conference Proceedings, Volume 801, pp. 196-199, astro-ph/0605489
- Butt, Y., et al. 2003, ApJ, 597, 494
- Butt, Y., et al., 2006, ApJ, 643, 238

Cesarsky, C. J. and Montmerle, T., 1983, Space Science Reviews, vol. 36, Oct. 1983, p. 173-193.

Chaty, S., & Rahoui, F., in Proceedings of The 6th INTEGRAL Workshop, The Obscured Universe, Space Research Institute, Moscow, Russia, July 2-8, 2006, to be published by ESA's Publications Division in December 2006 as Special Publication SP-622, astro-ph/0609474

Combi, J. A., et al., 2003, ApJ 588, 731

Dickey & Lockman, 1990, Annu. Rev. Astron. Astrophys., 28, 215

Domingo-Santamaria, E., & Torres, D., 2006, A&A 448, 613

Filliatre, P., & Chaty, S., 2004, ApJ, 616, 469

Georganopoulos, M., Perlman, E. & Kazanas, D., 2005 ApJL 634, 33

Grindlay, J., et al., 1975, ApJL 197, L9

Konopelko, A., et al. (VERITAS collaboration), 2006, ApJ, accepted – available on astro-ph

Lang, M.J., et al. 2004, A&A, 423, 415

Massey, P. & Thompson, A. B., 1991, Astron. J., 101, 1408

Monet, D. G., et al., 2003, AJ, 125, 984

Mukherjee, R., et al., 2003, ApJ, 589, 487

Mukherjee, R., et al., 2006, to appear in Proceedings of the conference "The Multi-Messenger Approach to High-Energy Gamma-ray Sources" Barcelona/Spain (2006), astro-ph/0610299

Paredes, J. M., 2006 "*High-energy gamma-ray emission in AGNs and microquasars*", Invited talk, to be published in the proceedings of the Vulcano Workshop 2006 "Frontier Objects in Astrophysics and Particle Physics", F. Giovannelli & G. Mannocchi (eds.), Italian Physical Society, Editrice Compositori, Bologna, Italy, astro-ph/0609168

Paredes, J. M., et al., 2006 ApJL accepted, astro-ph/0611881

Setia Gunawan, D. Y. A., et al., Ap J SS, 149, 123, 2003

Schoenmakers, A. P., 2001 "*Double-double radio galaxies: probing duty cycles in AGN and the cocoons of powerful radio sources*", in Particles and Fields in Radio Galaxies Conference, ASP Conference Proceedings Vol. 250. Edited by Robert A. Laing and Katherine M. Blundell. ISBN: 1-58381-090-0. San Francisco: Astronomical Society of the Pacific, p.408

Sreekumar, P., et al., 1999 Astroparticle Physics 11, 221

Taylor, A. R., et al., 1996 ApJS, 107, 239

Vlemmings, W. H. T., Cordes, J. M. and Chatterjee, S., 2004, ApJ 610, 402

Wendker, H. J., Higgs, L. A., and Landecker, T. L., 1991, A&A, 241, 551

Acknowledgements

YMB is supported by NASA/Chandra and NASA/INTEGRAL General Observer Grants and a NASA Long Term Space Astrophysics Grant. JPF and AK thank the US DOE for their continued support. JAC is a researcher of the program Ramon y Cajal funded jointly by the Spanish Ministerio de Ciencia y Tecnologia and Universidad de Jaen. J. C. also acknowledges support by DGI of the Spanish Ministerio de Educacion y Ciencia under grants AYA2004-07171-C02-02 and FEDER funds and Plan Andaluz de Investigacion of Junta de Andalucia as research group FQM322.

Figures

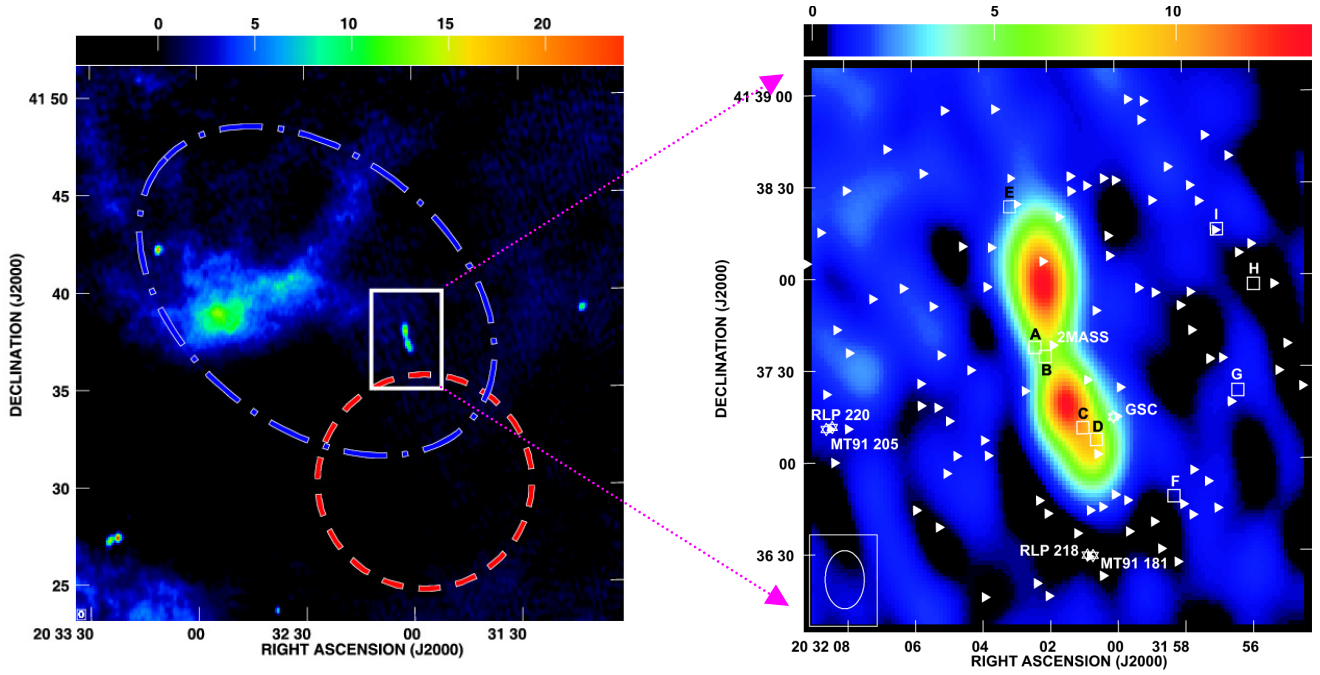


Figure 1: (left) 1400MHz WSRT map (made from data of Setia-Gunawan et al., 2003) showing the *approximate* location and extent of the Whipple TeV γ -ray hotspot (blue) as well as the extended HEGRA emission region (red). Note that the Whipple hotspot does not necessarily correspond to an extended TeV gamma-ray emission region but is simply the highest likelihood region of gamma-ray emission, of either a point-like nature or an intrinsically extended region of radius less than ~ 7 arcmin. The blue ellipse shown corresponds roughly to the 600 excess counts level in Fig 3 of Konopelko et al. (2006). Note the other two non-thermal radio sources, WSRTGP 2031+4116 (also dual-lobed; $\alpha_{2000}, \delta_{2000} = 20\ 33\ 23.19\ +41\ 27\ 23.7$), and WSRTGP 2031+4131 ($\alpha_{2000}, \delta_{2000} = 20\ 33\ 10.6\ +41\ 42\ 11$) can be seen towards the lower-left and upper left regions of the figure, respectively. The large region of diffuse radio emission towards the center of the Whipple hotspot location is thermal in nature (see text).

(right) A close-up of the dual-lobed non-thermal radio source of interest at 1.4GHz, overlaid w/ CHANDRA (\square) and 2MASS (\blacktriangleright) counterparts. CHANDRA sources have been labeled alphabetically. Stars are shown as (\star) and appear with their catalog names: it is likely that the close pairs of stars are in reality the same star which appear twice in the catalogs with slightly different coordinates. GSC refers to the star GSC 03161-00887.

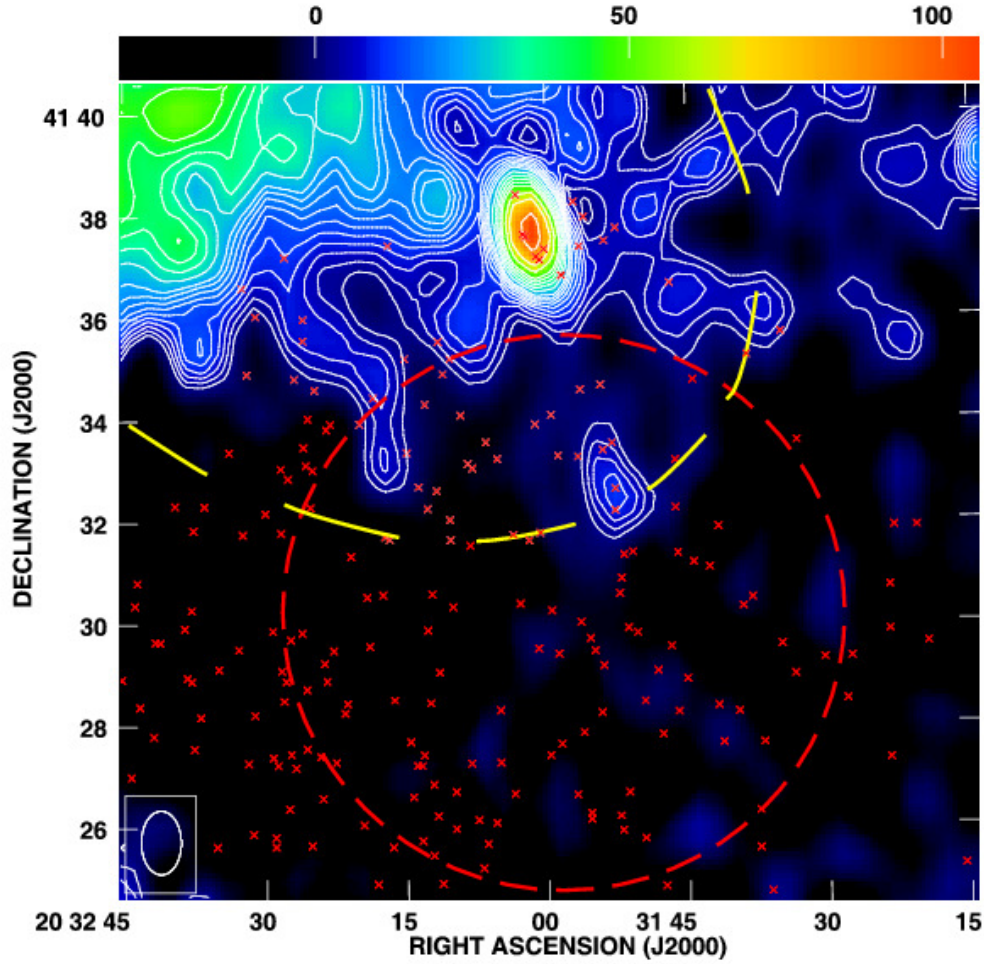


Figure 2: 365MHz WSRT data showing the diffuse non-thermal radio condensation at $\alpha_{2000}, \delta_{2000} = (20\ 31\ 53, +41\ 32\ 35)$ which is aligned with the radio-lobes and has a flux of $\sim 11.6\text{mJy}$ at 365 MHz. Since the resolution at 365 MHz is poorer than at 1400MHz the two lobes are not discernable in this image. CHANDRA X-ray sources are shown as red crosses, and the HEGRA (red) and Whipple (yellow) TeV emission regions are marked. Note that the CHANDRA field of view only covered part of the radio field displayed above.

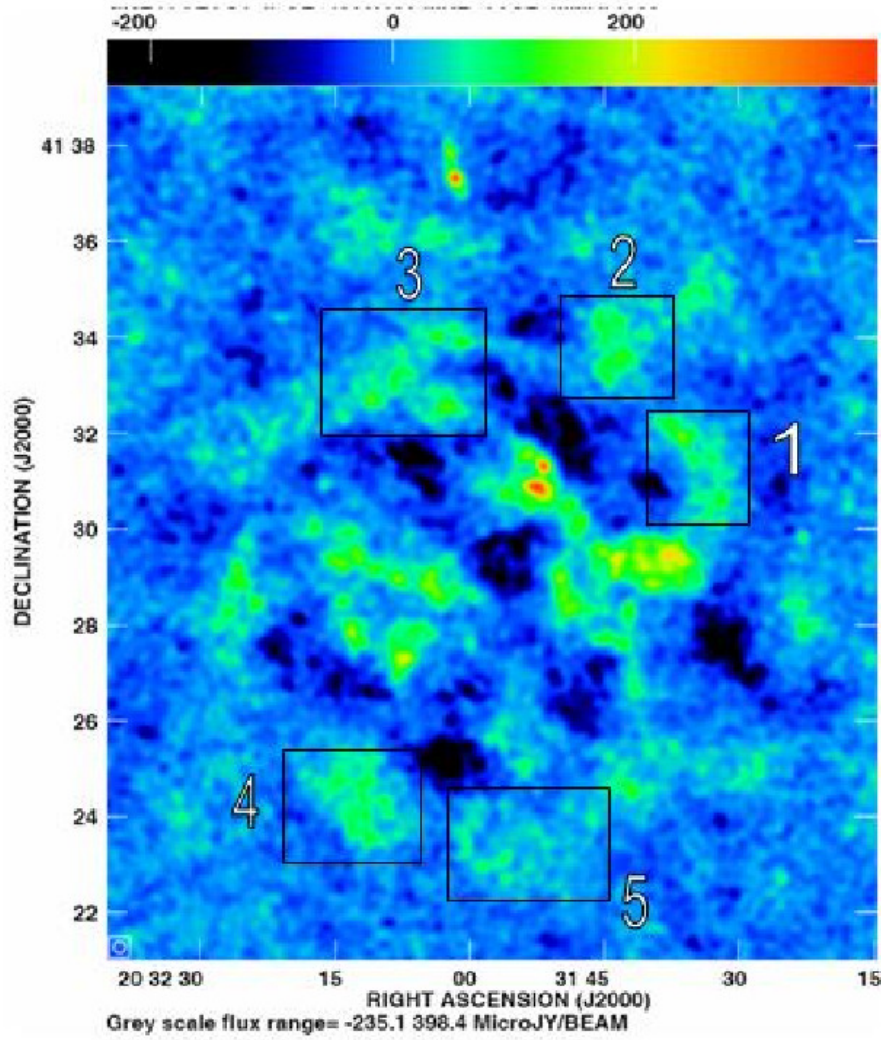


Figure 3: 4.8GHz VLA data taken 29 April 2003. The presence of a weak ring-like structure with center approximately $\alpha_{2000}, \delta_{2000} = (20\ 32\ 00, +41\ 29\ 30)$ and radius ~ 5 arcmin, consistent with the dimension reported by HEGRA, is evident. The dual-lobed radio source can also be seen to the north. The spectral index of the ring varies, with the western side in general being more non-thermal, with $\alpha \sim -1$. As the eastern side is not detected at 1.4GHz (with an rms noise level of ~ 0.5 mJy/beam), that region is likely thermal with an index of about $\alpha \sim +0.8$, or larger. Dividing the structure into the several regions shown above we have computed the fluxes and spectral indices as follows: Region 1 (center: 20 31 34.56, +41 31 14.66): $F(1.4\text{GHz}) = 9.7 \pm 0.7$ mJy and $F(4.8\text{GHz}) = 2.0 \pm 0.1$ mJy. $\alpha_1 \sim -1.29$. Region 2 (center: 20 31 44.17, +41 33 47.76): $F(1.4\text{GHz}) = 9 \pm 1$ mJy and $F(4.8\text{GHz}) = 2.7 \pm 0.1$ mJy. $\alpha_2 \sim -1.18$. Region 3 (center: 20 32 05.28, +41 33 17.78): $F(1.4\text{GHz}) = 7 \pm 1$ mJy and $F(4.8\text{GHz}) = 2.9 \pm 0.1$ mJy. $\alpha_3 \sim -0.63$. Region 4 (center: 20 32 11.66, +41 24 26.74): $F(1.4\text{GHz}) = 4.2 \pm 0.9$ mJy and $F(4.8\text{GHz}) = 2.8 \pm 0.1$ mJy. $\alpha_4 \sim -0.43$. Region 5 (center: 20 31 54.6, +41 23 26.8): $F(1.4\text{GHz}) = 19 \pm 0.8$ mJy and $F(4.8\text{GHz}) = 1.7 \pm 0.1$ mJy. $\alpha_5 \sim -1.8$. The errors on the spectral indices quoted are ~ 0.2 .